

University of Groningen

On the width of the recombination zone in ambipolar organic field effect transistors

Kemerink, M.; Charrier, D. S. H.; Smits, E. C. P.; Mathijssen, S. G. J.; de Leeuw, D. M.; Janssen, R. A. J.

Published in:
Applied Physics Letters

DOI:
[10.1063/1.2963488](https://doi.org/10.1063/1.2963488)

IMPORTANT NOTE: You are advised to consult the publisher's version (publisher's PDF) if you wish to cite from it. Please check the document version below.

Document Version
Publisher's PDF, also known as Version of record

Publication date:
2008

[Link to publication in University of Groningen/UMCG research database](#)

Citation for published version (APA):

Kemerink, M., Charrier, D. S. H., Smits, E. C. P., Mathijssen, S. G. J., de Leeuw, D. M., & Janssen, R. A. J. (2008). On the width of the recombination zone in ambipolar organic field effect transistors. *Applied Physics Letters*, 93(3), 033312-1-033312-3. [033312]. <https://doi.org/10.1063/1.2963488>

Copyright

Other than for strictly personal use, it is not permitted to download or to forward/distribute the text or part of it without the consent of the author(s) and/or copyright holder(s), unless the work is under an open content license (like Creative Commons).

The publication may also be distributed here under the terms of Article 25fa of the Dutch Copyright Act, indicated by the "Taverne" license. More information can be found on the University of Groningen website: <https://www.rug.nl/library/open-access/self-archiving-pure/taverne-amendment>.

Take-down policy

If you believe that this document breaches copyright please contact us providing details, and we will remove access to the work immediately and investigate your claim.

Downloaded from the University of Groningen/UMCG research database (Pure): <http://www.rug.nl/research/portal>. For technical reasons the number of authors shown on this cover page is limited to 10 maximum.

On the width of the recombination zone in ambipolar organic field effect transistors

M. Kemerink,^{1,a)} D. S. H. Charrier,¹ E. C. P. Smits,^{2,3} S. G. J. Mathijssen,^{1,2}
D. M. de Leeuw,^{2,3} and R. A. J. Janssen¹

¹Department of Applied Physics, Eindhoven University of Technology, P.O. Box 513,
5600 MB Eindhoven, The Netherlands

²Philips Research Laboratories, High Tech Campus 4, 5656 AE Eindhoven, The Netherlands

³Molecular Electronics, Zernike Institute of Advanced Materials, University of Groningen,
9700 AB Groningen, The Netherlands

(Received 9 June 2008; accepted 2 July 2008; published online 23 July 2008)

The performance of organic light emitting field effect transistors is strongly influenced by the width of the recombination zone. We present an analytical model for the recombination profile. By assuming Langevin recombination, the recombination zone width W is found to be given by $W = \sqrt{4.34d\delta}$, with d and δ the gate dielectric and accumulation layer thicknesses, respectively. The model compares favorably to both numerical calculations and measured surface potential profiles of an actual ambipolar device. © 2008 American Institute of Physics. [DOI: 10.1063/1.2963488]

The recent realization of bipolar currents in organic field effect transistors has enabled the fabrication of organic light emitting field effect transistors (LEFETs).¹ The high current densities in these devices² as compared to those in diode-type devices may help to reach population inversion, which is a prerequisite for an electrically driven organic laser.³ Apart from the possible use in an organic lasing device, LEFET may offer significant advantages over conventional organic light emitting diodes. Not only the high current density, but also the possibility to shift the recombination zone away from the metallic contacts and the fact that all free carriers contribute to exciton formation can lead to increased brightness and efficiency.^{1,4} However, the high carrier and exciton densities in LEFET may also enhance exciton quenching, reducing the internal quantum efficiency.^{2,4,5}

Since exciton-exciton and exciton-carrier quenching rates are strong functions of the exciton and carrier densities, both the maximum attainable exciton density and the internal and external quantum efficiencies of LEFET strongly depend on the width of the recombination zone. So far, the actual value of the recombination zone width W has received surprisingly little attention. In theoretical works, W is commonly taken to be zero, i.e., an infinite bimolecular recombination rate R is assumed.^{6–8} Experimentally, both confocal optical⁹ and electrostatic¹⁰ methods have been employed to resolve the recombination profile, yielding values for W in the micrometer range. However, both techniques suffer from a non-negligible finite spatial resolution.

Here, we present an analytical model for the width and shape of the recombination profile in ambipolar transistors, including LEFET.¹¹ The results compare favorably to numerical calculations and indicate that typically $W \approx 100$ nm when R is given by the Langevin rate. This observation is supported by a detailed analysis of surface potential profiles as measured by scanning Kelvin probe microscopy (SKPM).

The analytical model calculates the recombination of electrons and holes in the recombination zone of an ambipolar field effect transistor (FET). For this, we divide the device

in three regions as illustrated in Fig. 1. In the regions between the source and drain contacts and the recombination zone we apply the gradual channel approximation,¹² i.e., the hole and electron densities are given by $p = C[V(x) - V_g]$ and $n = C[V_g - V(x)]$, with $V(x)$ and V_g the (local) channel and gate potentials, respectively. $C = \epsilon_0 \epsilon_r / d$ is the gate capacitance with ϵ_r and d the relative dielectric constant and thickness, respectively, of the gate insulator. Inside the recombination zone we assume that the carrier densities are determined by the recombination process only. Assuming further a constant electrostatic field F , the hole and electron

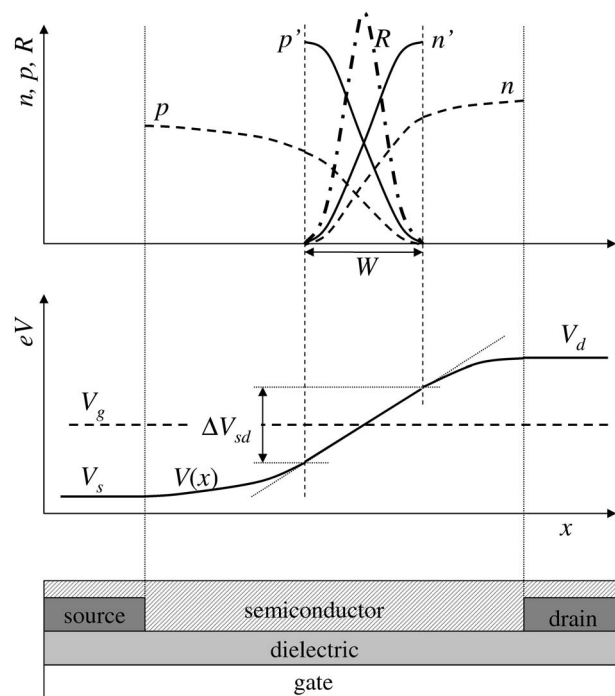


FIG. 1. Schematic layout of the LEFET as assumed in the analytical model. The top panel shows carrier densities and recombination vs position in the LEFET channel. The middle panel shows the potential profile, and the bottom panel the device layout. Parameters are explained in the text. Note that n' and p' are symmetric, whereas n and p are not.

^{a)}Electronic mail: m.kemerink@tue.nl.

drift current densities are $j_h = qp\mu_h F$ and $j_e = qn\mu_e F$, with q the elementary charge, p and n the hole and electron densities, respectively, and μ_h , μ_e the hole and electron mobilities, respectively. Using a Langevin-type recombination rate $R = \gamma np$, one finds the hole and electron densities as follows:

$$\frac{dp}{dt} = \frac{dp}{dx} \frac{dx}{dt} = \frac{dp}{dx} v_h = -\gamma np = \frac{dn}{dx} v_e = \frac{dn}{dt}, \quad (1)$$

where $v_h = \mu_h F$ and $v_e = -\mu_e F$ are the hole and electron drift velocities, respectively. In Eq. (1), diffusion effects are tacitly ignored, which will be justified below. Defining effective densities $p' \equiv \mu_h p$ and $n' \equiv \mu_e n$ current conservation demands that the limiting values of p' and n' on either side of the recombination zone are equal, i.e., $p'_0 = n'_0 = j/qF$. For a given source-drain voltage V_{sd} , this condition fixes the gate voltage to $V_s - V_g = V_{sd}/[1 + (\mu_h/\mu_e)]$, to be used later. Moreover, one has $p'(x) + n'(x) = p'_0 + n'_0$ everywhere in the recombination zone. With these definitions one easily arrives at the following differential equations:

$$\frac{dp'}{dx} = -\alpha p'(p'_0 - p') \quad \text{and} \quad \frac{dn'}{dx} = \alpha n'(n'_0 - n'), \quad (2)$$

with $\alpha \equiv \gamma/\mu_h\mu_e F$. Taking the source (drain) on the left (right) and for the source (V_s), gate (V_g), and drain (V_d) voltages $V_s > V_g > V_d$ as in Fig. 1, the solution of Eq. (2) is

$$p' = \frac{p'_0}{\exp[p'_0\alpha(x - x_0)] + 1} \quad \text{and} \quad n' = \frac{n'_0 \exp[n'_0\alpha(x - x_0)]}{\exp[n'_0\alpha(x - x_0)] + 1}, \quad (3)$$

with x_0 the position of the center of the recombination zone, where $p'(x_0) = n'(x_0) = 1/2 n'_0$. The recombination profile follows from $R = \gamma np$, i.e.,

$$R = \frac{\gamma n_0'^2}{\mu_h \mu_e} \frac{\exp[n'_0\alpha(x + x_0)]}{\{\exp[n'_0\alpha(x + x_0)] + 1\}^2}. \quad (4)$$

Taking W as the width at which R reaches $1/e$ of its maximum value, one obtains $W = 4.34/n'_0\alpha$.

In order to apply the above to actual devices, estimates for the boundary conditions p'_0 and n'_0 and the field F need to be made. Defining ΔV_{sd} as the voltage drop over the recombination zone, one finds from their definitions that $\alpha \sim 1/F = W/\Delta V_{sd}$ and $n'_0 \sim \Delta V_{sd}$. Hence $W = 4.34/n'_0\alpha$ becomes the square root of a constant, i.e., independent of ΔV_{sd} . The full expression for W is easiest obtained by setting $\Delta V_{sd} = V_{sd}$, i.e., $F = V_{sd}/W$. The gate bias determines p_0 according to $p_0 = (\epsilon_0 \epsilon_r / q d \delta)(V_s - V_g)$, with δ the thickness of the accumulation layer. Using $V_s - V_g = V_{sd}/[1 + (\mu_h/\mu_e)]$ as derived above from current conservation, and the Langevin¹³ value for the recombination prefactor $\gamma = q(\mu_h + \mu_e)/\epsilon_0 \epsilon_r$, one finally finds

$$W = \sqrt{4.34 d \delta}. \quad (5)$$

Typical values for δ are around 1–10 nm,¹⁴ and for d 50 nm–1 μm , giving W values in the range of 15–200 nm. The surprisingly few parameters in Eq. (5) reflect the cancellation of (a) the mobility dependence of the drift velocity and recombination rate, (b) the dielectric constant dependence of the capacitance and recombination rate, and (c) the bias dependence of the carrier density ($\sim V_g$) and drift velocity

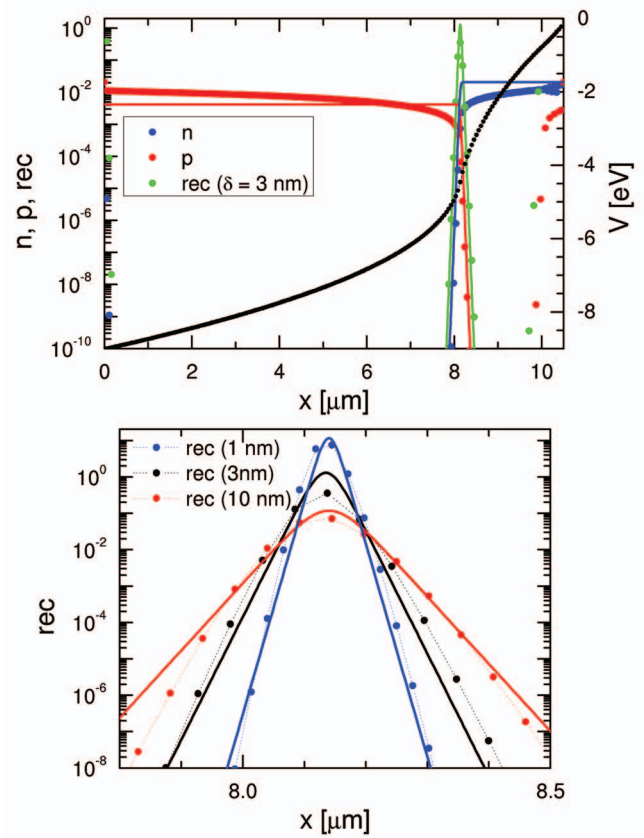


FIG. 2. (Color) Top: Electron and hole densities and recombination (left axis) and potential (right axis) vs position in the NiDT channel. Dots: numerical model; lines: Eqs. (3) and (4). n and p are normalized to the density of states, hence recombination is in units of s^{-1} . Parameters used are $\mu_h = 1 \times 10^{-11} \text{ m}^2/\text{V s}$, $\mu_e = 2 \times 10^{-12} \text{ m}^2/\text{V s}$, $\epsilon_r = 3.6$, $d = 240 \text{ nm}$, and $\delta = 3 \text{ nm}$. Bottom: Zoom-in of the recombination profile for $\delta = 1, 3$, and 10 nm . Symbols + dotted lines: numerical model; solid lines: Eq. (4).

($\sim V_{sd}$) since V_g and V_{sd} are linked by current conservation as discussed above.

Let us now briefly come back to the ignored effects of carrier diffusion. The broadening of the recombination profile due to diffusion can be estimated from $W_{\text{diff}} \approx \sqrt{D\tau}$. Here, D is the diffusion constant, linked to the mobility via the Einstein relation $D = \mu k_B T / q$, with k_B the Boltzmann constant and T the absolute temperature. The recombination time constant τ is estimated as $\tau \approx 1/\gamma n_0$. With this, W_{diff} becomes $W_{\text{diff}} \approx W \sqrt{k_B T / q V_{sd}}$. Since the square root term is much smaller than unity for all practical devices as $k_B T / q \approx 25 \text{ meV}$ at room temperature, diffusion broadening can, indeed, safely be ignored.

In Fig. 2, the predictions of Eqs. (3)–(5) are compared to numerical solutions of the coupled drift/diffusion and Poisson equations. The parameters used correspond to the nickel dithiolene (NiDT) devices described in Ref. 10. Clearly, both the height and shape of the recombination profile, and correspondingly the decay of the electron and hole densities, are accurately reproduced by the analytical model. In the bottom panel of Fig. 2, the numerically and analytically calculated recombination profiles for three different accumulation layer thicknesses are compared. Indeed, the numerically obtained profile has a width that follows Eq. (5). Note that the numerically calculated recombination profile is extremely sensitive to undersampling. Likely, this explains the large differences between the present results and those in Ref. 15. The larger

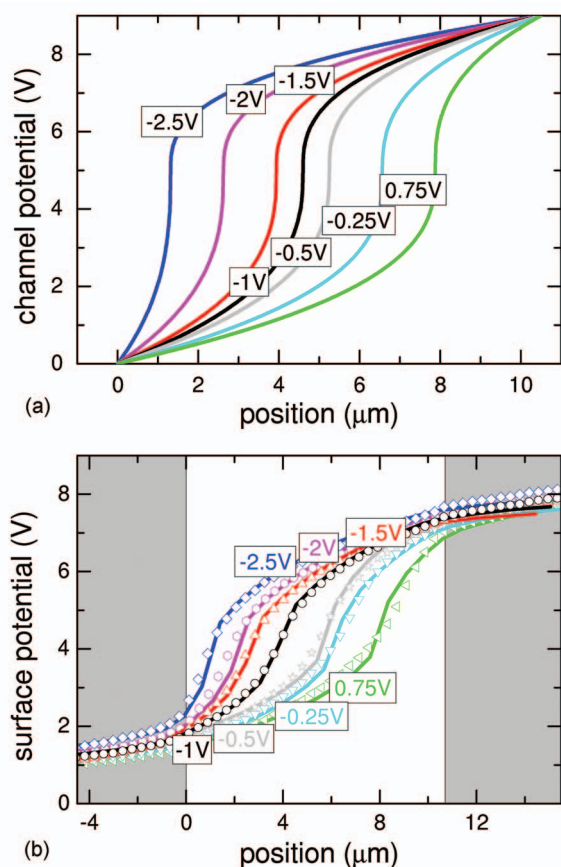


FIG. 3. (Color) (a) Potential profiles in the LEFET channel calculated from the analytical model and parameters of Ref. 10. The source-drain voltage is 9 V; the gate voltage is indicated at the corresponding curve. (b) Measured surface potential (symbols) and SKPM response calculated from the curves in (a) (lines).

widths found numerically by Smith and Ruden¹⁶ are due to a different choice of recombination prefactor.

As mentioned above, the finite spatial resolution of experimental probes prevents a direct comparison with experiments. In particular, the SKPM response is not solely due to the interaction between the tip apex and the underlying sample, but results from the complex three-dimensional (3D) interaction between the entire probe, consisting of cantilever, cone and apex, and the entire sample. We have used a recently developed model to take the full 3D electrostatics into account.¹⁷ These calculations contain no free parameters, both the main inputs being the (known) geometry of the tip and sample and the “true” surface potential. As input for the true surface potential we use the analytical expressions for $V(x)$ as derived by Smits *et al.* [see Fig. 3(a)].¹⁰ These calculations are based on variable range hopping in an exponential density of states, and assume $W=0$. The calculation of the surface potential takes only parameters as inputs that are

independently determined, i.e., the entire calculation is free of fitting parameters. The calculated surface potentials accurately match the measured ones [see Fig. 3(b)]. Within their error margins, the shapes of the experimental and numerical traces are equal. A detailed analysis of the calculated and measured surface potentials in the recombination region allows us to put an upper limit to W of less than $0.5 \mu\text{m}$.

In order to arrive at values for W that are in the micrometer range, as claimed by Swensen *et al.* on the basis of confocal microscopy experiments,⁹ the recombination prefactor needs to be set significantly below the Langevin value that is used in this paper. Reducing γ by a factor β ($\beta < 1$) leads to an increase in W by a factor $\beta^{-1/2}$.

Summarizing, we have presented an analytical model for the recombination profile in organic ambipolar FETs. The model only depends on experimentally easily accessible parameters and predicts a recombination zone width in the range of 15–200 nm, which is confirmed by numerical calculations. A detailed analysis of the surface potential obtained by SKPM on nickel dithiolenes devices supports the notion of a narrow recombination zone.

We gratefully acknowledge H. Sirringhaus and C. Groves for stimulating discussions. The work of E.S. is funded by the Dutch Polymer Institute (Project 516).

¹For a recent review see, e.g., J. Zaumseil and H. Sirringhaus, *Chem. Rev. (Washington, D.C.)* **107**, 1296 (2007).

²T. Takenobu S. Z. Bisri, T. Takahashi, M. Yahiro, C. Adachi, and Y. Iwasa, *Phys. Rev. Lett.* **100**, 066601 (2008).

³For a recent review see, e.g., I. D. W. Samuel and G. A. Turnbull, *Chem. Rev. (Washington, D.C.)* **107**, 1272 (2007).

⁴J. Zaumseil, R. H. Friend, and H. Sirringhaus, *Nat. Mater.* **5**, 69 (2006).

⁵S. Verlaak, D. Cheyns, M. Debuquoy, V. Arkhipov, and P. Heremans, *Appl. Phys. Lett.* **85**, 2405 (2004).

⁶D. L. Smith and P. P. Ruden, *Appl. Phys. Lett.* **89**, 233519 (2006).

⁷E. C. P. Smits, T. D. Anthopoulos, S. Setayesh, E. van Veenendaal, R. Coehoorn, P. W. M. Blom, B. de Boer, and D. M. de Leeuw, *Phys. Rev. B* **73**, 205316 (2006).

⁸R. Schmechel, M. Ahles, and H. von Seggern, *J. Appl. Phys.* **98**, 084511 (2005).

⁹J. S. Swensen, J. Yuen, D. Gargas, S. K. Buratto, and A. J. Heeger, *J. Appl. Phys.* **102**, 013103 (2007).

¹⁰E. C. P. Smits, S. G. J. Mathijssen, M. Cölle, A. J. G. Mank, P. A. Bobbert, P. W. M. Blom, B. de Boer, and D. M. de Leeuw, *Phys. Rev. B* **76**, 125202 (2007).

¹¹For this problem, only the capture rate of positive and negative charges matters; the question whether subsequent recombination is emissive or not is irrelevant. Hence the model is valid for any ambipolar FET.

¹²S. M. Sze, *Physics of Semiconductor Devices*, 2nd ed. (Wiley, New York, 1981).

¹³P. Langevin, *Ann. Chim. Phys.* **7**, 433 (1903).

¹⁴G. Horowitz, R. Hajlaoui, and P. Delannoy, *J. Phys. III* **5**, 355 (1995).

¹⁵G. Paasch, Th. Lindner, C. Rost-Bietsch, S. Karg, W. Riess, and S. Scheinert, *J. Appl. Phys.* **98**, 084505 (2005).

¹⁶D. L. Smith and P. P. Ruden, *J. Appl. Phys.* **101**, 084503 (2007).

¹⁷D. S. H. Charrier, M. Kemerink, B. E. Smalbrugge, T. de Vries and R. A. J. Janssen, *ACS Nano* **2**, 622 (2008).